Computers and Mathematics with Applications 61 (2011) 731–744

Contents lists available at ScienceDirect

Computers and Mathematics with Applications

journal homepage: www.elsevier.com/locate/camwa

Decentralized control of multi-agent systems for swarming with a given geometric pattern

Teddy M. Cheng *, Andrey V. Savkin

School of Electrical Engineering and Telecommunications, The University of New South Wales, Sydney, NSW 2052, Australia

ARTICLE INFO

Article history:
Received 31 July 2010
Received in revised form 12 November 2010
Accepted 15 November 2010

Keywords:
Multi-agent and autonomous systems
Collective behavior
Decentralized control

ABSTRACT

This paper addresses a problem of cooperative formation control of a network of self-deployed autonomous agents. We propose a decentralized motion coordination control for the agents so that they collectively move in a desired geometric pattern from any initial position. There are no predefined leaders in the group and only local information is required for the control. The control algorithm is developed using the ideas of information consensus, and its effectiveness is illustrated via numerical simulations.

© 2010 Elsevier Ltd. All rights reserved.

1. Introduction

Due to the advances in communication, sensing, micro-electronics, and computing technologies, it becomes more popular to deploy multi-agents or multi-robots in operations such as: object transportation [1]; localization and mapping [2]; and monitoring and coverage [3–7]. In order to achieve these operations, each agent in a multi-agent network requires to cooperate with each other in the network to fulfill a common goal. The cooperation takes place in the form of coordinated control among the agents using the information from the network. However, to reduce the cost of an operation, each agent may have very limited resources, e.g., communication or sensing powers. Therefore, a centralized control algorithm is not a practical approach since not all the global information is available to each agent. To circumvent the lack of global information, a decentralized approach should be considered.

The study of decentralized control laws for groups of autonomous agents has emerged as a challenging research area recently, e.g., [8–15]. In this control framework, the motion of each agent is coordinated using local information such as coordinates or velocities of several other agents that are closest neighbors of the agent at a given time. One approach to developing these local motions is by the inspiration from the animal aggregations, such as schools of fish, flocks of birds or swarms of bees, that are believed to use simple, local motion coordination rules at the individual level (e.g., [16–20]). To simulate these behaviors, Vicsek et al. [21] proposed a simple discrete-time model of a system of several autonomous agents and each agent's motion is updated using a local rule based on its own state and the state of its "neighbors". This simple but interesting model was then analytically analyzed by a number of researchers, e.g., [8,22,23,9,24,25]. Moreover, modifications of the Vicsek model have also been carried out in, e.g., [24–27]. For example, the Vicsek model with adaptive velocities was proposed in [26,27]; whereas the heterogeneous sensing Vicsek model was introduced in [28]. In addition, the converging rate of the Vicsek model was studied in [24,25].

The basic feature of the Vicsek model is the local coordination rules or the nearest neighbor rules. These types of rules in turn form a basis to the so-called consensus or agreement scheme (see, e.g., [8,11,12,9,15]). By using this scheme, a group of agents can coordinate to achieve, e.g., a specific formation or geometric structure. One of the advantages of

* Corresponding author. Tel.: +61 2 93854778; fax: +61 2 9385993.
E-mail addresses: t.cheng@ieee.org (T.M. Cheng), a.savkin@unsw.edu.au (A.V. Savkin).

0898-1221/$ – see front matter © 2010 Elsevier Ltd. All rights reserved.
doi:10.1016/j.camwa.2010.11.023

this consensus approach as compared to, for example, the traditional leader–follower approach (e.g., [29,30]) is that a leader–follower scheme requires a predefined leader. Since there is no explicit feedback to the leader from the formation in the leader–follower scheme and the leader moves independently, the leader may walk away and leave its followers behind. However, the attractiveness of using this leader–follower scheme is that a formation coordination problem can simply be reformulated as a typical regulation or tracking control problem.

Instead of assigning a leader in the group, the concept of virtual leader was also adopted in formation control. Using a virtual leader, for instance in [14], a decentralized control law for the formation control or stabilization of a group of unicycles was proposed. The control law proposed in [14] requires that the inter-vehicle communication graph be fixed and the neighbors of each agent are the same for all time; whereas the communication graph in a typical consensus scheme can be time-varying. In other words, the neighbors of an agent may vary over time in a consensus scheme. Another approach that is widely adopted for formation control is the artificial potential function approach (e.g., [31,32]). As its name suggests, this approach is based on some potential functions, and these functions represent and realize the inter-agent interactions and/or the interactions with the environment. An advantage of this approach is that it requires less information to be communicated among agents and naturally leads to a distributed control law. However, most potential function based algorithms suffer from the fact that it is difficult to guarantee the convergence to the desired formation pattern.

By taking the consensus approach, the objective of this paper is to develop a decentralized or distributive control strategy for a group of agents so that they form a given geometric pattern and collectively move in this pattern from any initial position. For brevity, we focus on the rectangular pattern in this paper. However, our control strategy can be modified to achieve other geometric patterns such as triangular or diamond patterns. In our problem, there are no leaders assigned *a priori*, and the agents have to coordinate with each other in the group relying on some global consensus in order to achieve and maintain a rectangular pattern. Potential applications of our formation control of a group of agents are for sweep coverage [4] in operations like minesweeping [33], boarder patrolling [34], environmental monitoring of disposal sites on the deep ocean floor [35], and sea floor surveying for hydrocarbon exploration [36].

The rest of the paper is organized as follows. In Section 2, we formulate the problem of decentralized formation control of a network of mobile agents. Algorithms to address the formation control problem are developed and presented in Section 3. Section 4 presents some simulation results to illustrate the proposed algorithm. Finally, some concluding remarks are given in Section 5.

2. Problem formulation

In our decentralized formation control problem, the objective is to coordinate a group of autonomous agents so that they form a rectangular lattice pattern and collectively move in this pattern from any initial deployment. The coordinating algorithms are decentralized such that the agents can only access local information. We consider a multi-agent system consisting of n agents labeled 1 through n. Let $V_i(\cdot)$ and $\Theta_i(\cdot)$ be the speed and heading of the agent i, respectively. Also, let $l(s) = [\cos(s)\ \sin(s)]^T$ be a unit vector with a given angle $s \in \mathbb{R}$ measured with respect to x-axis and let $p_i = [x_i, y_i]^T$ be the position of the agent i. For a given sampling period $T > 0$, the discrete-time kinematic equations of the agents are given by:

$$p_i((k+1)T) = p_i(kT) + V_i(kT)l(\Theta_i(kT))T, \tag{1}$$

for $i = 1, 2, \dots, n$, $k = 0, 1, 2, \dots$. The speed V_i satisfies $|V_i(kT)| \le v_{\max}$ for $i = 1, 2, \dots, n$ and all $k \ge 0$. The initial headings satisfy $\Theta_i(0) \in [0, \pi)$ for all $i = 1, 2, \dots, n$, and the initial positions of the agents are in a bounded set $\mathcal{B} \subset \mathbb{R}^2$ with Lebesgue measure.

Agent i, $i = 1, 2, \dots, n$, has the ability to communicate with other agents that are in a disk of radius r defined by

$$D_{i,r}(kT) := \{p \in \mathbb{R}^2 : \|p - p_i(kT)\| \le r\},$$

where $\|\cdot\|$ denotes the Euclidean norm. Let $\mathcal{N}_i(kT)$ be the set of all agents $j, j \ne i$ that at time $t = kT$ belong to the disk $D_{i,r}(kT)$ and $|\mathcal{N}_i(kT)|$ be the number of elements in $\mathcal{N}_i(kT)$. We describe that the agent i has $|\mathcal{N}_i(kT)|$ number of *neighbors* at time kT. Let $\mathcal{P}$ be the collection of simple undirected graphs defined on n vertices, representing agents $1, 2, \dots, n$. For any time $kT \ge 0$, the relationships between neighbors are described by a simple undirected graph $G(kT) \in \mathcal{P}$ with vertex set $\{1, 2, \dots, n\}$ where i corresponds to the agent i. The vertices i and j of the graph, where $i \ne j$, are connected by an edge if and only if the agents i and j are neighbors at time kT. To study our problem, we impose the following assumption on $G(kT)$.

Assumption 2.1. The graph $G(kT) \in \mathcal{P}$ is connected for all $k \ge 0$.

For any integers $\gamma, \bar{K} \in \{1, 2, \dots, n\}$ and scalars $\bar{\psi}, \bar{\phi} \in [0, \pi)$, and $s_1, s_2 > 0$, we define a number points $h_{i,j}(kT)$ relative to agent γ at time kT as shown in Fig. 1. The set of locations $\{h_{i,j}(kT)\}$ is defined as follows:

$$h_{i,j}(kT) = p_\gamma(kT) + s_2(i-1)l(\bar{\phi}) + s_1(j-1)l(\bar{\phi} - \pi/2) \tag{2}$$

for $i = 1, 2, \dots, \lfloor n/\bar{K} \rfloor$ and $j = 1, 2, \dots, \bar{K}$; and for $i = \lceil n/\bar{K} \rceil$ and $j = 1, 2, \dots, n - \lfloor n/\bar{K} \rfloor \bar{K}$. The $h_{i,j}(kT)$ positions are relative to the position of agent γ. In fact, the integer $\gamma \in \{1, 2, \dots, n\}$ is not specified at the initial deployment and any agent can eventually take up the $h_{1,1}(kT)$ position. Similarly, the integer $\bar{K}$ and scalar $\bar{\phi}$ are also unspecified at the initial deployment. Thus, the dimensions and the orientation of the rectangular lattice are unknown *a priori*. Moreover, the heading

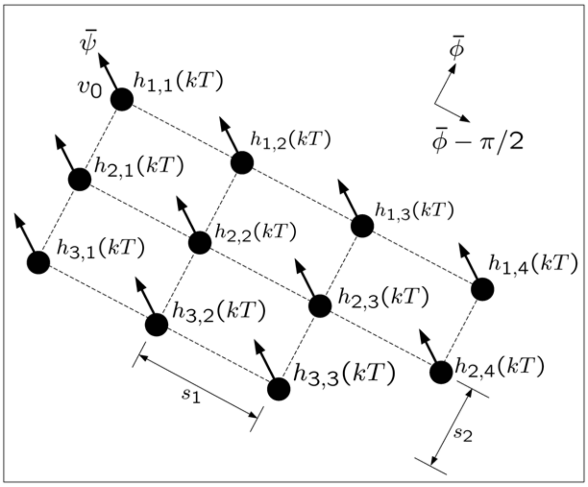

Fig. 1. A group of agents moving in the rectangular formation with speed v_0 and heading $\bar{\psi}$ ($n = 11$, $\bar{K} = 4$).

$\bar{\psi}$ of the rectangular lattice is also not specified at the initial deployment. However, the desired speed at which the group of agents should move is known to all the agents. We let v_0 be such a desired speed at which the group of agents should move.

Definition 2.1. Given n autonomous agents, a set of decentralized control algorithms is said to be a rectangular formation control for the agents if for almost all initial agent positions, there exist an agent $\gamma \in \{1, 2, \dots, n\}$, integer $\bar{K} \in \{1, 2, \dots, n\}$, and scalars $\bar{\phi}, \bar{\psi} \in [0, \pi)$; and for each $h_{i,j}(kT)$ location, there exists a unique index $z_{i,j} \in \{1, 2, \dots, n\}$ such that the following condition holds:

$$\lim_{k\to\infty} \|p_{z_{i,j}}(kT) - h_{i,j}(kT)\| = 0. \tag{3}$$

In Definition 2.1, almost all means for all initial conditions except for a set of initial conditions has Lebesgue measure (area) zero.

3. Algorithms

In this section, a set of control algorithms will be presented for the coordination of a group of moving agents to achieve a rectangular formation. In brief, the algorithms consist of two stages. During the first stage, the agents coordinate and align themselves into a line formation. Once the agents are aligned and each has been assigned an identity (ID) based on this line formation, they start forming $\lceil n/\bar{K} \rceil$ number of parallel lines. The distance between these lines is s_2. Depending on $\bar{K}$ and n, the last row of agents may not form a complete line as shown in Fig. 1.

3.1. First stage

In the following, a set of decentralized control laws will be proposed for the agents to use in the first stage. In this stage, the objective is to steer the agents such that they achieve a line formation as shown in Fig. 2(b) from any initial position (see Fig. 2(a)). Since the control laws for the agents are distributed or decentralized, they rely on the local information of each agent. Information such as locations and coordination variables of an agent's neighbors is available to the agent. The coordination variables are for coordinating the motion of an agent with other agents in the group.

First, for agent i ($i = 1, 2, \dots, n$), we introduce the coordination variable $K_i(kT)$ that takes a value in the discrete set $\{1, 2, \dots, n\}$. The initial value of this variable satisfies $K_i(0) \in \{1, 2, \dots, n\}$. This coordination variable will characterize the dimensions of the triangular lattice that the agents will form, in particular, the number of agents along one side of a rectangular pattern. At any time $k = 1, 2, 3, \dots$, agent i updates $K_i(kT)$ using the following "nearest neighbor rule". Let $\mathcal{A}_i(t)$ be the average of $K_i(kT)$ at time kT, namely,

$$\mathcal{A}_i(kT) := \frac{1}{1 + |\mathcal{N}_i(kT)|}\left(K_i(kT) + \sum_{j\in\mathcal{N}_i(kT)} K_j(kT)\right). \tag{4}$$

It is clear that $\mathcal{A}_i(kT) \in [1, n]$. Now we define the update rule for $K_i(\cdot)$ of agent i as follows:

$$K_i((k+1)T) := \lfloor \mathcal{A}_i(kT) \rfloor. \tag{5}$$

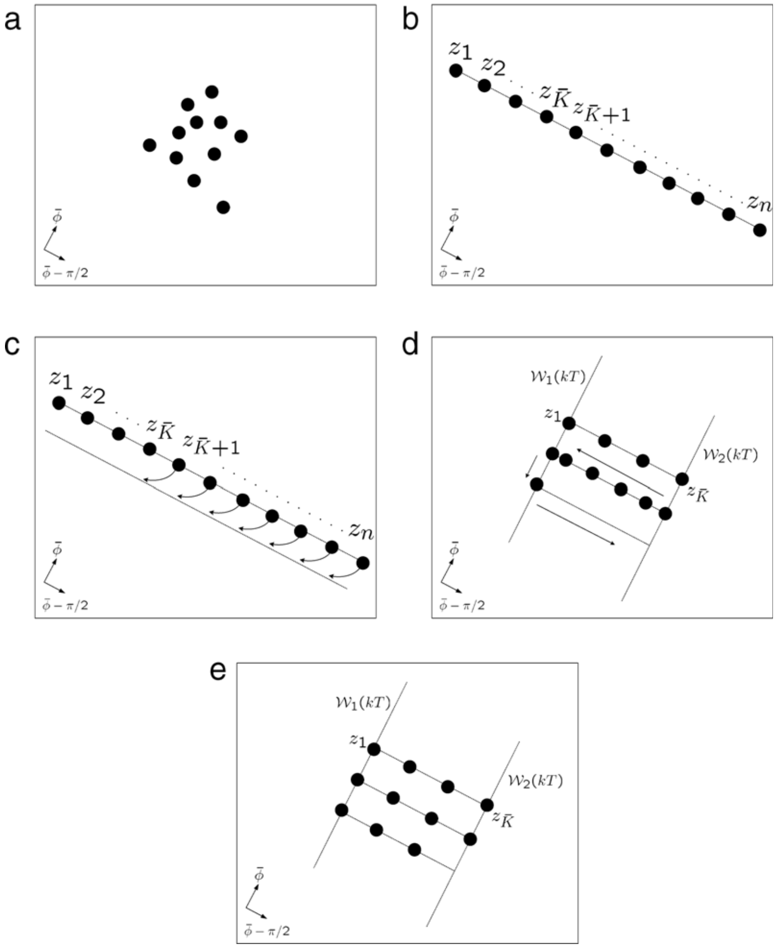

Fig. 2. Agents' relative positions: (a) initial deployment; (b) after stage 1; (c) at the beginning of stage 2; (d) during stage 2; and (e) rectangular pattern formed ($n = 11, \bar{K} = 4$).

Next we introduce the coordination variable $\psi_i(kT)$ for agent *i*. This variable will be used to define the heading of the final rectangular formation. The coordination variable $\psi_i(kT)$ has initial value $\psi_i(0) = \Theta_i(0)$. The variable $\psi_i(\cdot)$ is also updated as follows:

$$\psi_i((k+1)T) := \frac{1}{1 + |\mathcal{N}_i(kT)|} \left(\psi_i(kT) + \sum_{j \in \mathcal{N}_i(kT)} \psi_j(kT) \right). \tag{6}$$

In addition, we introduce the variable $\xi_i(kT) \in \{1, 2, 3 \ldots\}$ with $\xi_i(0) = 1$. This variable characterizes the row in the formation that agent *i* belongs to at time kT. It is clear that during the first stage, $\xi_i(\cdot) \equiv 1$. At time kT, we define a set $\mathcal{S}_i(kT) = \{j \in \mathcal{N}_j(kT) : \xi_j(kT) = \xi_i(kT)\}$. The set $\mathcal{S}_i(kT)$ contains the neighbors of agent *i* that belong to the same row as agent *i*. Similar to $\psi_i(kT)$, another coordination variable $\phi_i(kT)$ for $i = 1, 2, \ldots, n$ is introduced and it will define the orientation of the rectangular formation. The coordination variable $\phi_i(kT)$ has initial value $\phi_i(0) \in [0, \pi)$, and we define:

$$\mathcal{H}_i(kT) := \frac{1}{1 + |\mathcal{S}_i(kT)|} \left(\phi_i(kT) + \sum_{j \in \mathcal{S}_i(kT)} \phi_j(kT) \right), \tag{7}$$

for $i = 1, 2, \ldots, n$, where $|\mathcal{S}_i(kT)|$ denotes the number of elements in the set $\mathcal{S}_i(kT)$. The coordination variable $\phi_i(kT)$ is updated by

$$\phi_i((k+1)T) = \mathcal{H}_i(kT). \tag{8}$$

In contrast to $K_i((k+1)T)$, the variables $\psi_i((k+1)T)$ and $\phi_i((k+1)T)$ will take any value in the interval $[0, \pi)$ rather than from a discrete set. Using $\phi_i(kT)$, we define a variable that is the projection of the position of agent *j*, i.e. $p_j(kT)$, in the direction $\phi_i(kT)$ as follows:

$$c_{i,j}(kT) = l^T(\phi_i(kT))p_j(kT), \tag{9}$$

for $j \in \mathcal{S}_i(kT) \cup \{i\}$.

Similar to (7), we define the average of $c_{i,j}(\cdot), j \in \mathcal{S}_i(kT) \cup \{i\}$ for agent i as follows:

$$\mathcal{M}_i(kT) := \frac{1}{1 + |\mathcal{S}_i(kT)|} \left(c_{i,i}(kT) + \sum_{j \in \mathcal{S}_i(kT)} c_{i,j}(kT) \right), \tag{10}$$

for $k = 1, 2, \ldots$. For each agent i, we introduce the coordination variable $\mathcal{F}_i(kT) = c_{i,i}(kT)$. Using $\phi_i(kT)$ and $\mathcal{F}_i(kT)$, a line $\mathcal{L}_i(kT)$ that agent i belongs to at time kT is defined as:

$$\mathcal{L}_i(kT) = \{p \in \mathbb{R}^2 : l^T(\phi_i(kT))p = \mathcal{F}_i(kT)\} \tag{11}$$

for $i = 1, 2, \ldots, n$ and $k = 0, 1, 2, \ldots$.

This line is instrumental in determining the control for agent i. To develop the control action along $\mathcal{L}_i(kT)$, we let $q_j^i(kT)$ be the projection of the position of agent $j \in \mathcal{S}_i(kT) \cup \{i\}$ on the line $\mathcal{L}_i(kT)$ at time kT, and it is given by $q_j^i(kT) = l^T(\phi_i(kT) - \pi/2)p_j(kT)$. Using this, for any agent i, we define its neighboring agents $\alpha, \beta \in \mathcal{S}_i(kT)$, provided that if they exist,

$$q_\alpha^i(kT) < q_i^i(kT) < q_\beta^i(kT). \tag{12}$$

During the first stage, if both agents α and β exist for agent i, then we define

$$\mathcal{Q}_i(kT) = \frac{q_\alpha^i(kT) + q_\beta^i(kT)}{2}. \tag{13}$$

If α exists but not β, then we define

$$\mathcal{Q}_i(kT) = \frac{q_\alpha^i(kT) + q_i^i(kT) + s_1}{2}. \tag{14}$$

On the other hand, if β exists but not α, then we define

$$\mathcal{Q}_i(kT) = \frac{q_\beta^i(kT) + q_i^i(kT) - s_1}{2}. \tag{15}$$

Before introducing our decentralized control laws, we define

$$\begin{aligned} \bar{v}_i(kT) &= (\mathcal{Q}_i(kT) - q_i^i(kT))/T \\ \hat{v}_i(kT) &= (\mathcal{M}_i(kT) - \mathcal{F}_i(kT))/T \end{aligned} \tag{16}$$

for $i = 1, 2, \ldots, n$ and $k = 1, 2, \ldots$. Using (16), we introduce the following variables:

$$\begin{aligned} v_i(kT) &= \sqrt{\bar{v}_i(kT)^2 + \hat{v}_i(kT)^2}; \\ \theta_i(kT) &= \begin{cases} \phi_i(kT) + \xi_i(kT) - \pi/2, & \text{if } \hat{v}_i(kT) \geq 0 \\ \phi_i(kT) - \xi_i(kT) - \pi/2, & \text{if } \hat{v}_i(kT) < 0, \end{cases} \end{aligned} \tag{17}$$

where $\xi_i(kT) := \cos^{-1}(\bar{v}_i(kT)/v_i(kT))$. Now we are in a position to present a set of decentralized control laws that is described by:

$$V_i(kT)\Theta_i(kT) = v_i(kT)l(\theta_i(kT)) + v_0 l(\psi_i(kT)). \tag{18}$$

3.2. Second stage

The first stage of the algorithm presented previously will drive the group of agents into a line formation. However, our objective is to drive the agents into a rectangular lattice pattern as shown in Fig. 1. Therefore, the purpose of the second stage of the algorithm is to meet this objective and will be presented in this subsection.

As mentioned in Section 2, the dimensions and the orientation $\bar{\phi}$ of the rectangular lattice are not predefined. In fact, these parameters will only be known to the agents when a global consensus is reached via sharing of local information. The control (18) guarantees that all agents will be aligned and moving in a line formation under the connectivity Assumption 2.1. In other words, the coordination variables have reached their respective consensus values. In addition, using rule (4), the variable $K_i(\cdot)$ will also reach a consensus value $\bar{K}$ that belongs to the discrete set $\{1, 2, \ldots, n\}$, i.e., $K_i(\cdot) = \bar{K}$ for $i = 1, 2, \ldots, n$. The value $\bar{K}$ will characterize the number of agents in each row of the final formation. Once the agents are aligned and $K_i(kT)$ has reached a consensus value $\bar{K}$, the leftmost agent initiates a counting sequence and the agents then count from the leftmost agent to the rightmost agent. By doing so, each agent has a unique number or ID defined by $N_i \in \{1, 2, \ldots, n\}$ that characterizes its location counted from the leftmost agent. By letting the leftmost agent be agent γ and the rightmost agent be δ, we have $N_\gamma = 1$ and $N_\delta = n$ and the agents between them from left to right have numbers from 2 to $n - 1$. As long as the rightmost agent has $N_\delta = n$ (meaning that all the agents have been assigned IDs), the algorithm moves to the second stage. In other words, just before moving to the second stage, there exists a set $\{z_1, z_2, \dots, z_n\}$, that is a permutation of the set $\{1, 2, \dots, n\}$, such that agent $z_1 = \gamma$ is at the leftmost position of the line, agent z_2 is at the right hand side of agent z_1, and so on. Therefore, the right most position is taken by the agent $z_n = \delta$.

During the second stage, agents that have their IDs N_i greater than $\bar{K}$ will move down to form a number of lines that are parallel to the first line of agents (see Fig. 2(c)–(d)). The distance between these lines is s_2. At the beginning of the second stage, the position of agent $z_{\bar{K}}$ is passed to agent z_n via agents $z_{\bar{K}+1}, \dots, z_{n-1}$. Agent z_n uses this information and moves to the position that is below agent $z_{\bar{K}}$ with distance s_2 between them. At the same time, agents $z_{\bar{K}+1}, z_{\bar{K}+2}, \dots, z_{n-1}, z_n$ set their variable $\xi_i(\cdot)$ to 2 (since they start forming a second layer of agent array).

To drive agent z_n below agent $z_{\bar{K}}$ with distance s_2, agent z_n uses the following rules:

$$\begin{aligned} \mathcal{Q}_{z_n}(kT) &= \begin{cases} (q_{z_n}(kT) + q_{z_{n-1}}(kT))/2, & \text{if } q_{z_{n-1}}(kT) > q_{z_{\bar{K}}(kT)}, \\ (q_{z_n}(kT) + q_{z_{\bar{K}}}(kT))/2, & \text{otherwise.} \end{cases} \\ \mathcal{M}_{z_n}(kT) &= (\mathcal{F}_{z_n}(kT) + c_{z_n,\bar{K}}(kT) - s_2)/2, \end{aligned} \tag{19}$$

where $c_{z_n,\bar{K}}(\cdot) = l^T(\phi_{z_n}(\cdot))p_{\bar{K}}(\cdot)$. By using (19), the position of agent z_n will satisfy

$$\lim_{k\to\infty} (p_{z_{\bar{K}}}(kT) - p_{z_n}(kT)) = s_2 l(\bar{\phi}). \tag{20}$$

At the same time, agents $z_{\bar{K}+1}, z_{\bar{K}+2}, \dots, z_{n-1}$ will follow agent z_n to go below agents $z_1, z_2, \dots, z_{\bar{K}}$ since $\xi_{z_{\bar{K}+1}}(\cdot), \xi_{z_{\bar{K}+2}}(\cdot), \dots, \xi_{z_n}(\cdot)$ are all set to 2. In addition, there will be a distance of s_2 separating these two rows of agents. Using algorithms that are similar to the ones developed for stage 1, agents $z_{\bar{K}+1}, z_{\bar{K}+2}, \dots, z_{n-1}$ will start to align themselves forming a second layer of agents that is parallel to the first one.

If $n = 2\bar{K}$, the number of agents in the second row will equal to $\bar{K}$ and a rectangular formation is achieved. On the other hand, if $n > 2\bar{K}$, the number of agents in the second row will exceed $\bar{K}$ and a rectangular pattern cannot be achieved, since there will be $n - 2\bar{K}$ excess agents that will move beyond agent z_1. One way to achieve the configuration as shown in Fig. 1 is that the $n - 2\bar{K}$ excess agents move down in the direction of $-l(\bar{\phi})$ below agent z_1, instead of moving beyond agent z_1. Once these agents have moved down, they again can start forming the third layer of agents. Similarly, if $n = 3\bar{K}$, three rows of agents will be formed and each row has $\bar{K}$ number of agents in it. However, if $n > 3\bar{K}$, the $n - 3\bar{K}$ excess agents will move down in the direction of $-l(\bar{\phi})$ below agent z_n. By repeating this process, there will be $\lfloor n/\bar{K} \rfloor$ number of rows formed with $\bar{K}$ number of agents in each row. For the last row, i.e., row $\lceil n/\bar{K} \rceil$, there will be $n - \lfloor n/\bar{K} \rfloor \bar{K}$ number of agents in it, as illustrated in Fig. 2(e).

In order to achieve the objective of the second stage, we need to modify $\bar{v}_i(\cdot)$ and $\hat{v}_i(\cdot)$ for agents that have IDs greater than $\bar{K}$ (i.e., agents that are not in the first row). After reaching the second stage, we will define two imaginary lines $\mathcal{W}_1(kT)$ and $\mathcal{W}_2(kT)$ that represent the sides of a rectangle orientated in the direction of $l(\bar{\phi})$. As shown in Fig. 2(d), these two parallel lines can be defined as

$$\begin{aligned} \mathcal{W}_1(kT) &:= \{p \in \mathbb{R}^2 | (p - p_{z_1}(kT))^T l(\bar{\phi} - \pi/2) = 0\} \\ \mathcal{W}_2(kT) &:= \{p \in \mathbb{R}^2 | (p - p_{z_{\bar{K}}}(kT))^T l(\bar{\phi} - \pi/2) = 0\}. \end{aligned} \tag{21}$$

The distance between these lines is $(\bar{K} - 1)s_1$.

Using these lines, we first consider the case when the variable $\xi_i(kT)$ of agent i is even (i.e., the even row). If both neighboring agents α and β of agent i exist as defined by (12), and $p_\alpha(kT) \notin \mathcal{W}_1(kT)$ or $p_\beta(kT) \notin \mathcal{W}_2(kT)$, then we use $\mathcal{Q}_i(kT)$ in (13) for agent i. If β exists but not α, or if β exists and α is on $\mathcal{W}_1(kT)$, then $\mathcal{Q}_i(kT)$ is defined by (15). If α exists but not β, then $\mathcal{Q}_i(kT)$ is defined by (14). If agent i hits $\mathcal{W}_1(kT)$ and there are no other agents in $\mathcal{S}_i(kT)$ that are on $\mathcal{W}_1(kT)$, agent i is then placed at $\mathcal{W}_1(kT)$ and $\mathcal{Q}_i(kT) = q^i_{\eta,1}(kT)$, where $q^i_{\eta,1}(kT) = l^T(\phi_i(kT) - \pi/2)\eta_{i,1}(kT)$ and $\eta_{i,1}(kT) := \mathcal{L}_i(kT) \cap \mathcal{W}_1$. When agent i moves along the line $\mathcal{W}_2(kT)$ from row $\xi_i(kT) - 1$ and agents α and β do not exist, then agent i is placed at $\mathcal{W}_2(kT)$ and define $\mathcal{Q}_i(kT) = q^i_{\eta,2}(kT)$, where $q^i_{\eta,2}(kT) = l^T(\phi_i(kT) - \pi/2)\eta_{i,2}(kT)$ and $\eta_{i,2}(kT) := \mathcal{L}_i(kT) \cap \mathcal{W}_2$.

Next, for the case with odd $\xi_i(kT)$ and $\xi_i(kT) \neq 1$, we can define $\mathcal{Q}_i(kT)$ for agent i in a similar manner as for the case with even $\xi_i(kT)$. If both agents α and β exist, and $p_\alpha(kT) \notin \mathcal{W}_1(kT)$ or $p_\beta(kT) \notin \mathcal{W}_2(kT)$, $\mathcal{Q}_i(kT)$ is defined by (13). If α exists but not β, or if α exists and β is on $\mathcal{W}_2$, then $\mathcal{Q}_i(kT)$ is defined by (14). On the other hand, if β exists but not α, then $\mathcal{Q}_i(kT)$ is defined by (15). If agent i hits $\mathcal{W}_2(kT)$ and there are no other agents in $\mathcal{S}_i(kT)$ that are on $\mathcal{W}_2(kT)$, agent i is placed at $\mathcal{W}_2(kT)$ and we define $\mathcal{Q}_i(kT) = q^i_{\eta,2}(kT)$. When agent i moves along $\mathcal{W}_1(kT)$ from line $\xi_i(kT) - 1$ and agents α and β do not exist, then agent i is placed at $\mathcal{W}_1(kT)$ and we define $\mathcal{Q}_i(kT) = q^i_{\eta,1}(kT)$.

If agent i is the agent placed at $\mathcal{W}_1(kT)$ and $\xi_i(kT)$ is odd and not equal to 1, or at $\mathcal{W}_2(kT)$ and $\xi_i(kT)$ is even, then we define $\bar{S}_i(kT)$, γ_i and $\bar{\mathcal{M}}_i(kT)$ such that

$$\begin{aligned} &\bar{\mathcal{S}}_i(kT) := \{j \in \mathcal{N}_i(kT) \mid \xi_j(kT) = \xi_i(kT) - 1\}; \\ &\gamma_i := \arg\min_{j\in\bar{\mathcal{S}}_i(kT)} |l^T(\phi_i(kT))(p_j(kT) - p_i(kT))|; \\ &\bar{\mathcal{M}}_i(kT) := \left(c_{i,\gamma_i}(kT) + c_{i,i}(kT) - s_2\right)/2. \end{aligned} \tag{22}$$

The value $\bar{\mathcal{M}}_i(kT)$ is for maintaining the distance between 2 rows of agents at s_2. Using $\mathcal{M}_i(kT)$, $\bar{\mathcal{M}}_i(kT)$ and $\mathcal{F}_i(kT)$, we introduce

$$\hat{\mathcal{M}}_i(kT) = \begin{cases} \mathcal{F}_i(kT) - s_2, & \text{if } \mathcal{Q}_i(kT) < q^i_{\eta,1}(kT) \\ & \text{or } \mathcal{Q}_i(kT) > q^i_{\eta,2}(kT) \\ \bar{\mathcal{M}}_i(kT), & \text{if } p_i(kT) \in \mathcal{W}_1 \text{ or } \mathcal{W}_2; \\ \mathcal{M}_i(kT), & \text{otherwise,} \end{cases} \tag{23}$$

and also

$$\hat{\mathcal{Q}}_i(kT) = \begin{cases} q^i_i(kT), & \text{if } \mathcal{Q}_i(kT) < q^i_{\eta,1}(kT) \\ & \text{or } \mathcal{Q}_i(kT) > q^i_{\eta,2}(kT) \\ \mathcal{Q}_i(kT), & \text{otherwise.} \end{cases} \tag{24}$$

To update the row number, we have

$$\xi_i((k+1)T) = \begin{cases} \xi_i(kT), & \text{if } q^i_{\eta,1}(kT) < \mathcal{Q}_i(kT) < q^i_{\eta,2}(kT); \\ \xi_i(kT) + 1, & \text{otherwise.} \end{cases} \tag{25}$$

Using $\hat{\mathcal{M}}_i(kT)$ and $\hat{\mathcal{Q}}_i(kT)$, we modify $\bar{v}_i(kT)$ and $\hat{v}_i(kT)$ in (16) as follows:

$$\begin{aligned} \bar{v}_i(kT) &= (\hat{\mathcal{Q}}_i(kT) - q^i_i(kT))/T \\ \hat{v}_i(kT) &= (\hat{\mathcal{M}}_i(kT) - \mathcal{F}_i(kT))/T. \end{aligned} \tag{26}$$

Again the control law for agent i is described by (17)–(18).

3.3. Main result

Theorem 3.1. *Consider n agents and their dynamics are described by Eq. (1). Suppose that Assumption 2.1 holds. Then the decentralized control (16), (18) and (26) is a rectangular formation control for the agents.*

Proof. See the Appendix. □

4. Simulation results

In this section, we first present two numerical simulations to illustrate the proposed algorithm. In the first simulation, a group of agents ($n = 19$) forms a rectangular formation with the consensus value $\bar{K} = 5$ and moves in the consensus direction of $\bar{\psi} = 1.433$ as shown in Fig. 3. It is clear that all the agents are aligning during the first stage (see Fig. 3(a) and (b)). Fig. 3(b) shows that the agents are aligned and ready to switch to the second stage. In the second stage (see Fig. 3(c)–(f)), the agents start forming a rectangular pattern by coordinating themselves following the strategy as shown in Fig. 2. In Fig. 3(c), the agents form into two rows only. As time proceeds, three rows and then four rows of agents are formed as illustrated in Fig. 3(d) and (e), respectively. In Fig. 3(e), even though the last row (i.e. the fourth row) of agents have already formed, the distance between agents in this row is not the same as that in rows one, two and three. At time $k = 380$ as shown in Fig. 3(f), this distance becomes consistent with that of the previous rows and from this time on, the agents will maintain and collectively move in the rectangular formation as defined in Definition 2.1. Since $n = 19$ and the consensus value $\bar{K} = 5$, there are only four agents, rather than five, in the last row as seen in Fig. 3(f). Fig. 4(a) and (b) show the speed $V_i(\cdot)$ and heading $\Theta_i(\cdot)$ profiles of the agents ($i = 1, 2, \dots, 19$), and they display that these values converged. In other words, all the agents moved in the same direction ($\bar{\psi} = 1.433$) with the same speed ($v_0 = 0.01$).

In the first simulation, the consensus values $\bar{\psi}$, $\bar{\phi}$ and $\bar{K}$ are unknown to all the agents *a priori*. In other words, at the initial deployment, the agents have no prior knowledge of the heading of the swarm, the orientation of the rectangular formation and the number of agents in each row, respectively. In the second simulation, we consider $n = 40$ agents. They are required to move in the given direction of $\pi/4$, and to form a rectangular pattern with a specified orientation of $\pi/4$ and with five rows. To achieve this, we simply set $\psi_1(\cdot) \equiv \pi/4$, $\phi_1(\cdot) \equiv \pi/4$ and $K_1(\cdot) \equiv 8$. As shown in Fig. 5, the group of agents ($n = 40$) formed five rows with $\bar{K} = 8$. The agents form a prefect rectangular pattern with the orientation of $\pi/4$ and the same number of agents in each row. Also, the group of agents moves in the direction of $\pi/4$. Fig. 6(a) and (b) show the velocity $V_i(\cdot)$ and heading $\Theta_i(\cdot)$ profiles of the agents ($i = 1, 2, \dots, 40$), and again they show that all the agents moved in the same direction ($\bar{\psi} = \pi/4$) with the same speed ($v_0 = 0.01$).

The proposed algorithms assume that the locations of agents are exactly known. In practice, there are a number of techniques that can be adopted for obtaining reliable position measurements like robust Kalman filtering (see, e.g.: [37,38]). To address the position measurement noise, a strategy to handle cycling under corrupted measurements is proposed below. Theorem 3.1 implies that there exists $\bar{\psi}$ such that $\lim_{k\to\infty} |\Theta_i(k) - \bar{\psi}| = 0$ and $\lim_{k\to\infty} |V_i(kT) - v_0| = 0$, for $i = 1, 2, \dots, n$, i.e. all agents eventually move in the direction of the consensus heading $\bar{\psi}$ with a given speed v_0. Using a similar argument, it is straightforward to show that if there are bounded uncertainties in the position measurements, there exist a finite time T_e

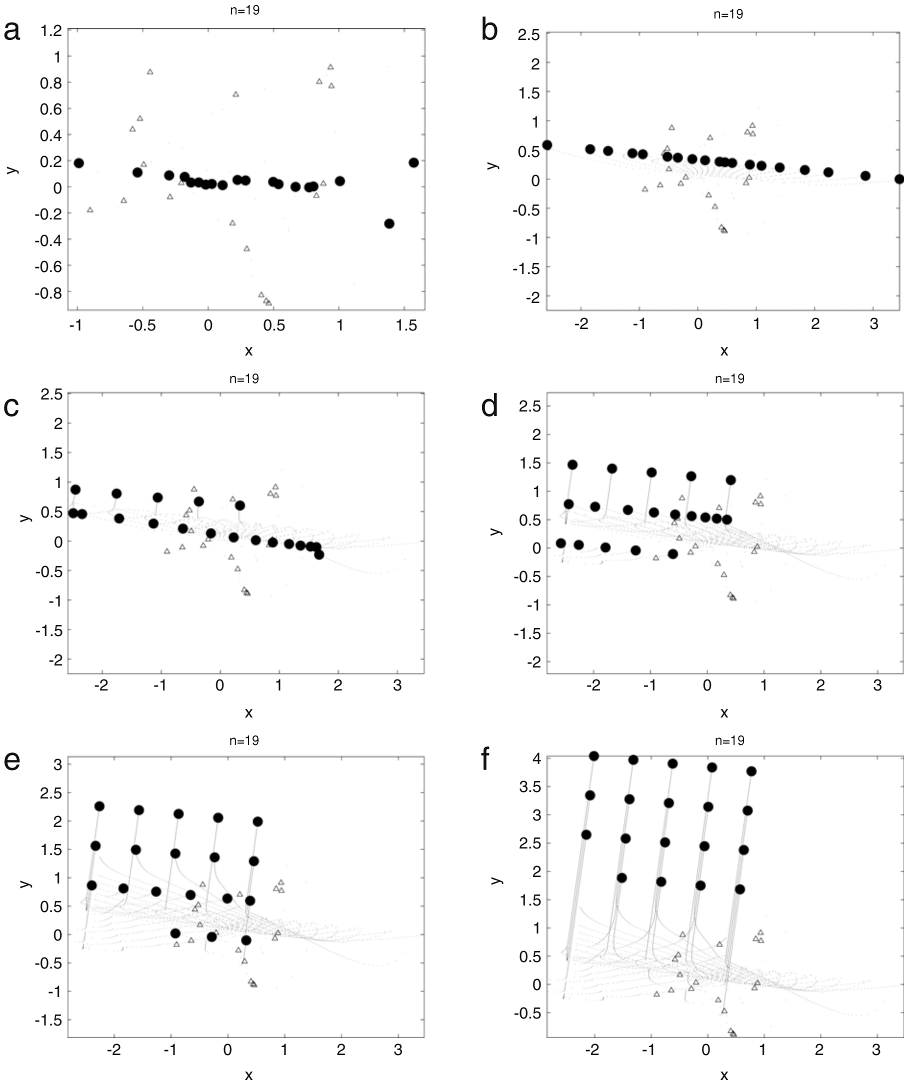

Fig. 3. Rectangular formation ($n = 19$) with $\bar{K} = 5$ and the agent positions ($\triangle$ representing $k = 0$) at: (a) $k = 3$; (b) $k = 30$; (c) $k = 60$; (d) $k = 120$; (e) $k = 240$; and (f) $k = 380$.

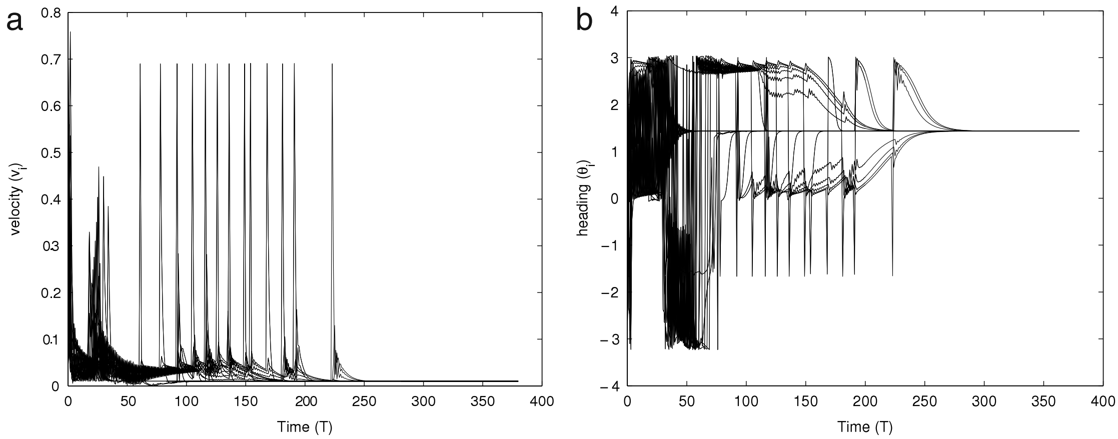

Fig. 4. (a) The speed V_i; and (b) the heading Θ_i of all agents ($n = 19$).

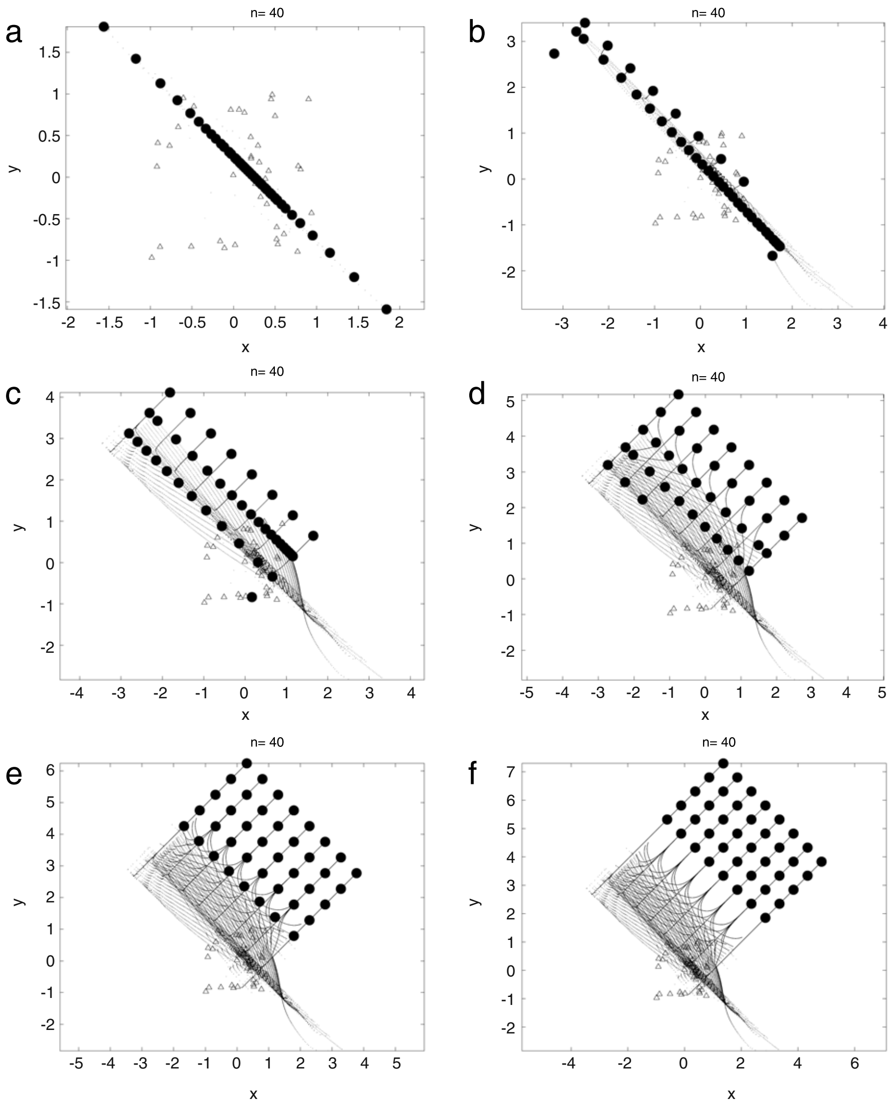

Fig. 5. Rectangular formation ($n = 40$) with desired $\bar{\psi}$, $\bar{\phi}$ and $\bar{K}$, and the agent positions ($\triangle$ representing $k = 0$) at: (a) $k = 10$; (b) $k = 100$; (c) $k = 300$; (d) $k = 600$; (e) $k = 900$; and (f) $k = 1200$.

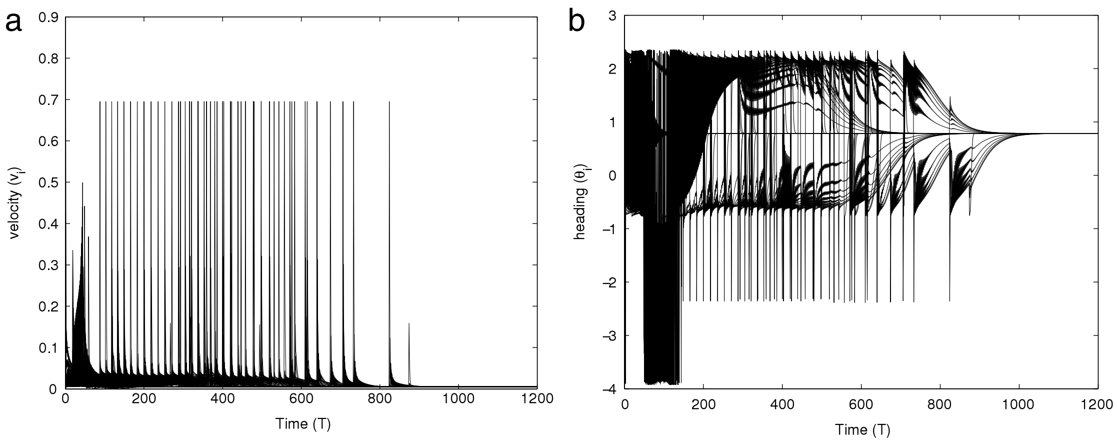

Fig. 6. (a) The speed V_i; and (b) the heading Θ_i of all agents ($n = 40$) with desired $\bar{\psi}$, $\bar{\phi}$ and $\bar{K}$.

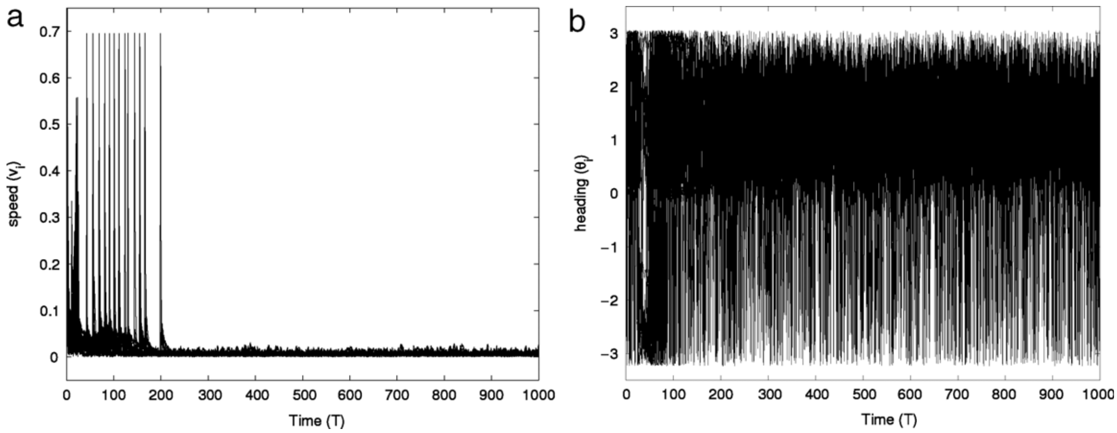

Fig. 7. (a) The speed V_i; and (b) the heading Θ_i of all agents ($n = 19$) with noisy position measurements.

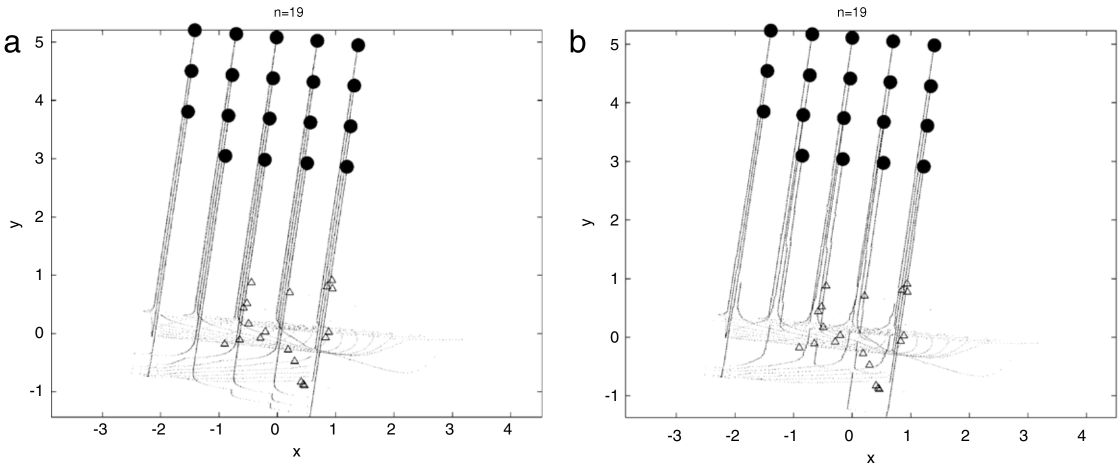

Fig. 8. Rectangular formation ($n = 19$) with $\bar{K} = 5$ and the agent positions ($\triangle$ representing $k = 0$) at $k = 1000$: (a) without cycling attenuation strategy; (b) with cycling attenuation strategy.

and a scalar ϵ_e such that $|V_i(kT) - v_0| \le \epsilon_e$ for all $k \ge k_e$ and $i = 1, 2, \ldots, n$. However, $V_i(kT)$ and also $\Theta_i(kT)$ may oscillate or cycle around v_0 and $\bar{\psi}$, respectively. The effect of cycling can be seen in a simulation study shown in Fig. 7(a) and (b); whereas Fig. 8(a) shows the agent formation. By observing Fig. 7(a) and (b), it is clear that the heading and the speed of each agent oscillate around $\bar{\psi} = 1.422$ and the given speed $v_0 = 0.005$, respectively. In this simulation, the position measurement noise is additive and described by $\varepsilon_i(t)$ such that the position of each agent is given by $(x_i(kT) + \varepsilon_i(kT), y_i(kT) + \varepsilon_i(kT))$, where $\varepsilon_i(kT)$ is uniformly distributed in the bounded interval $[-0.005, 0.005]$.

To attenuate the effect of cycling, we propose the following strategy. Since $|V_i(kT) - v_0| \le \epsilon_e$ for all $k \ge k_e$, one can choose $v_e < \epsilon_e$ and if $|v_i(kT) - v_0| \le v_e$, then

$$V_i(kT) = v_0 \quad \text{and} \quad \Theta_i(kT) = \psi_i(kT). \tag{27}$$

The desired speed v_0 is known to all the agents; whereas by consensus the coordination variable $\psi_i(kT)$ satisfies $\psi_i(kT) \to \bar{\psi}$. By using this strategy and setting $v_e = 0.009$, cycling is attenuated as shown in Figs. 9(a) and (b) and 8(b) shows the corresponding agent formation. The speed and heading of the agents in this simulation with cycling attenuation strategy are in sharp contrast to those obtained without the strategy as shown in Fig. 7(a) and (b). In other words, by using the above strategy, the formation is less sensitive to position measurement noise and as a result, it is more steady.

5. Conclusions

In this paper, a decentralized formation control was developed to coordinate a group of autonomous agents so that they collectively move into a rectangular lattice pattern from any initial deployment. The control was developed using the consensus approach and it requires only local information. Numerical simulations were performed to illustrate the control algorithm. To address the limitations of the current results, issues such as collision avoidance between agents, obstacle avoidance, and physical constraints of the agents are currently under investigation.

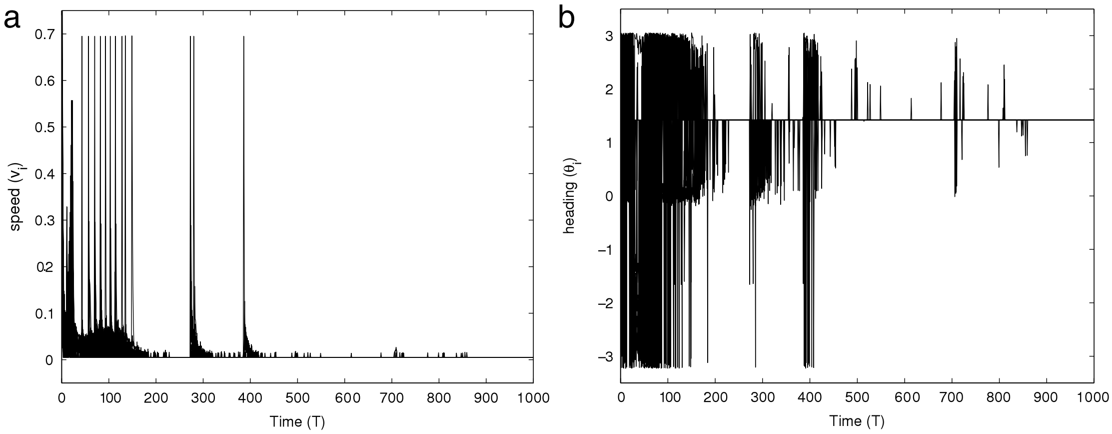

Fig. 9. (a) The speed V_i; and (b) the heading Θ_i of all agents ($n = 19$) with noisy position measurements using cycling attenuation strategy.

Acknowledgement

This work was supported by the Australian Research Council.

Appendix

Proof of Theorem 3.1. We will show it in terms of two stages. For the first stage, agent i has initial condition $\{p_i(0), \theta_i(0), \psi_i(0), \phi_i(0), K_i(0)\}$, for $i = 1, 2, \ldots, n$. The connectedness property imposed in Assumption 2.1 and the update laws for ϕ_i, ψ_i, K_i guarantee that there exist $\bar{\psi}, \bar{\phi} \in [0, \pi)$ and $\bar{K} \in \{1, 2, \ldots, n\}$ such that

$$\lim_{k\to\infty} \psi_i(kT) = \bar{\psi}, \qquad \lim_{k\to\infty} \phi_i(kT) = \bar{\phi}, \qquad \lim_{k\to\infty} K_i(kT) = \bar{K}, \tag{28}$$

for $i = 1, 2, \ldots, n$ (see, e.g., [8,22,9]). In other words, agents $1, 2, \ldots, n$ reach a consensus in terms of the variables $\psi_i(\cdot)$, $\phi_i(\cdot)$ and $K_i(\cdot)$. Using $\bar{\psi}$, we define the following system

$$\hat{p}((k+1)T) = \hat{p}(kT) + v_0 T l(\bar{\psi}) \tag{29}$$

with $\hat{p}(0) = 0$ and write $p(kT)$ as follows:

$$p_i(kT) = \bar{p}_i(kT) + \hat{p}(kT) \tag{30}$$

for $i = 1, 2, \ldots, n$, and $k = 0, 1, 2, \ldots$, where the state $\bar{p}_i(kT)$ is governed by

$$\bar{p}_i((k+1)T) = \bar{p}_i(kT) + T l(\theta_i(kT)) + w_i(kT), \tag{31}$$

where $w_i(kT) := T v_0 (l(\psi_i(kT)) - l(\bar{\psi}))$.

Next, we consider system (31) and suppose that the algorithm does not switch to the second stage. By using (16), we will show that there exist a scalar $\bar{\mathcal{F}}_1$ and a fixed line

$$\bar{\mathcal{L}}_1 = \{p \in \mathbb{R}^2 : p^T l(\bar{\phi}) = \bar{\mathcal{F}}_1\} \tag{32}$$

such that

$$\lim_{k\to\infty} d(\bar{p}_i(kT), \bar{\mathcal{L}}_1) = 0, \quad i = 1, 2, \ldots, n, \tag{33}$$

where $d(\bar{p}_i(\cdot), \bar{\mathcal{L}}_0)$ is defined as the distance between the point $\bar{p}(\cdot)$ and the line $\bar{\mathcal{L}}_0$. Moreover, for a given $s_1 > 0$, there exists a set $\{z_1, z_2, \ldots, z_n\}$ that is a permutation of the set $\{1, 2, \ldots, n\}$ such that

$$\lim_{k\to\infty} \|\bar{p}_{z_i}(kT) - \bar{p}_{z_1}(kT)\| = (i-1)s_1, \tag{34}$$

for $i = 1, 2, \ldots, n$.

First, using the facts that $\lim_{k\to\infty} \|w_i(kT)\| = 0$ and $\lim_{k\to\infty} \phi_i(kT) = \bar{\phi}$, there exists a scalar $\bar{\mathcal{F}}_1$ such that $\lim_{k\to\infty} \mathcal{F}_i(kT) = \bar{\mathcal{F}}_1$ for $i = 1, 2, \ldots, n$. By the definition of $\mathcal{F}_i$ and the property that $\lim_{k\to\infty} \phi_i(kT) = \bar{\phi}$, condition (33) holds.

To show condition (34), at time kT, we define the largest distance $d_{\max}(kT)$ from the line $\bar{\mathcal{L}}_1$ to $\bar{p}_i(kT)$ by

$$d_{\max}(kT) := \max_{i=1,2,\ldots,n} d(\bar{p}_i(kT), \bar{\mathcal{L}}_1). \tag{35}$$

For a given $\delta > 0$, condition (33) implies that there exists $\mathcal{J}_1 \geq 0$ such that $d_{\max}(kT) < \delta$, for all $k \geq \mathcal{J}_1$, and there also exists a set $\{z_1^{(1)}, z_2^{(1)}, \dots, z_n^{(1)}\}$ that is a permutation of the set $\{1, 2, \dots, n\}$ such that the projections of the positions of agents $z_1^{(1)}, z_2^{(1)}, \dots, z_n^{(1)}$ on the line $\bar{\mathcal{L}}_1$ satisfy the following condition:

$$q_{z_1^{(1)}}(kT) < q_{z_2^{(1)}}(kT) < \cdots < q_{z_n^{(1)}}(kT) \tag{36}$$

for all $k \geq \mathcal{J}_1$, where

$$q_{z_i^{(1)}}(kT) := [\sin(\bar{\phi}) \quad -\cos(\bar{\phi})]^T \times \bar{p}_{z_i^{(1)}}(kT); \tag{37}$$

for $i = 1, 2, \dots, n$. The rules for $\mathcal{Q}_i(kT)$ that govern $q_{z_1^{(1)}}(kT), q_{z_2^{(1)}}(kT), \dots, q_{z_n^{(1)}}(kT)$, can be written as a linear dynamic system

$$q^{(1)}((k+1)T) = A^{(1)} q^{(1)}(kT) + b^{(1)}, \quad \text{for } k \geq \mathcal{J}_1, \tag{38}$$

where

$$q^{(1)}(kT) := \begin{bmatrix} q_{z_2^{(1)}}(kT) - q_{z_1^{(1)}}(kT) \\ q_{z_3^{(1)}}(kT) - q_{z_2^{(1)}}(kT) \\ \vdots \\ q_{z_{n-1}^{(1)}}(kT) - q_{z_{n-2}^{(1)}}(kT) \\ q_{z_n^{(1)}}(kT) - q_{z_{n-1}^{(1)}}(kT) \end{bmatrix}, \qquad b^{(1)} := \begin{bmatrix} s_1/2 \\ 0 \\ \vdots \\ 0 \\ s_1/2 \end{bmatrix}$$

and $A^{(1)}$ is a square matrix with elements $A_{i,j}^{(1)}$, $1 \leq i, j \leq n-1$ such that $A_{i,i+1}^{(1)} = A_{i+1,i}^{(1)} = 1/2$, for $1 \leq i \leq n-1$; and $A_{i,j}^{(1)} = 0$, for all other i, j. By using the result [39, p. 514], it can be shown that $\lim_{k\to\infty} q^{(1)}(kT) = s_1 \mathbb{1}$, where $\mathbb{1} = [1\ 1\ \dots\ 1]^T$ and hence,

$$\lim_{k\to\infty} (q_{z_i^{(1)}}(kT) - q_{z_1^{(1)}}(kT)) = (i-1)s_1 \tag{39}$$

for $i = 1, 2, \dots, n$. Since $\lim_{k\to\infty} d(\bar{p}_i(kT), \bar{\mathcal{L}}_1) = 0$, we therefore have

$$\lim_{k\to\infty} (\bar{p}_{z_i^{(1)}}(kT) - \bar{p}_{z_1^{(1)}}(kT)) = (i-1)s_1 l(\bar{\phi} - \pi/2). \tag{40}$$

Therefore, for the first layer, there exists a set

$$Z^{(1)} := \{z_1^{(1)}, z_2^{(1)}, \dots, z_{\bar{K}}^{(1)}\} \subset \{1, 2, \dots, n\} \tag{41}$$

such that $\lim_{k\to\infty} \|p_{z_j^{(1)}}(kT) - h_{1,j}(kT)\| = 0$, for $j = 1, 2, \dots, \bar{K}$, since $z_1^{(1)} = \gamma$.

So far we have showed that if the algorithm does not switch to the second stage, the agents will be in a line formation with heading $\bar{\psi}$ and the distance between agents in this line formation is s_1. On the other hand, when the second stage is activated, our proposed algorithms drive the agents that have IDs greater than $\bar{K}$ (i.e., agents $z_{\bar{K}+1}^{(1)}, z_{\bar{K}+2}^{(1)}, \dots, z_n^{(1)}$) to form a number of parallel layers of agents, and the distance between layers is s_2.

As discussed before, if $n \geq 2\bar{K}$, the $\bar{K}$ of the excess $n - \bar{K}$ agents will then form a second layer of agent array. We will repeat the above argument, but in the opposite direction below agent $\bar{K}$, to show that $\bar{K}$ of the $n - \bar{K}$ number of agents converge to $h_{2,1}(kT), h_{2,2}(kT), \dots, h_{2,\bar{K}}(kT)$ relative to agent γ. By following the procedure used for the first layer, there exists a line

$$\bar{\mathcal{L}}_2 = \{p \in \mathbb{R}^2 : l^T(\bar{\phi})p = l^T(\bar{\phi})(\bar{\mathcal{F}}_1 - s_2)\},$$

an integer $\mathcal{J}_2 \geq \mathcal{J}_1$, and a set

$$Z^{(2)} := \{z_1^{(2)}, z_2^{(2)}, \dots, z_{\bar{K}}^{(2)}\} \subset \{1, 2, \dots, n\} \setminus Z^{(1)}$$

that is a permutation of the set $\{1, 2, \dots, n\} \setminus Z^{(1)}$ such that

$$\lim_{k\to\infty} d(\bar{p}_{z_i^{(2)}}(kT), \bar{\mathcal{L}}_2) = 0, \quad i \in \{1, 2, \dots, \bar{K}\} \tag{42}$$

and

$$q_{z_1^{(2)}}(kT) > q_{z_2^{(2)}}(kT) > \cdots > q_{z_{n-n_1}^{(2)}}(kT) \tag{43}$$

for all $k \geq \mathcal{J}_2$.

Agent $z_1^{(2)}$ is below and connects with agent $z_{\bar{K}}^{(1)}$, and the location of this agent is the starting point for forming the second layer of agent array. Similar to (38), we can write a linear dynamic system

$$q^{(2)}((k+1)T) = A^{(2)}q^{(2)}(kT) + b^{(2)}(kT), \quad \text{for } k \geq \mathcal{J}_2, \tag{44}$$

where

$$q^{(2)}(kT) := \begin{bmatrix} q_{z_1^{(2)}}(kT) - q_{z_2^{(2)}}(kT) \\ q_{z_2^{(2)}}(kT) - q_{z_3^{(2)}}(kT) \\ \vdots \\ q_{z_{\bar{K}-2}^{(2)}}(kT) - q_{z_{\bar{K}-1}^{(2)}}(kT) \\ q_{z_{\bar{K}-1}^{(2)}}(kT) - q_{z_{\bar{K}}^{(2)}}(kT) \end{bmatrix}, \qquad b^{(2)} := \begin{bmatrix} s_1/2 \\ 0 \\ \vdots \\ 0 \\ s_1/2 \end{bmatrix}$$

and $A^{(1)}$ is a square matrix with elements $A_{i,j}^{(1)}$, $1 \leq i, j \leq \bar{K} - 1$ such that $A_{i,i+1}^{(1)} = A_{i+1,i}^{(1)} = 1/2$, for $1 \leq i \leq \bar{K} - 1$; and $A_{i,j}^{(1)} = 0$. We have

$$\lim_{k\to\infty} (\bar{p}_{z_1^2}(kT) - \bar{p}_{z_i^{(2)}}(kT)) = (i-1)s_1 l(\bar{\phi} - \pi/2), \tag{45}$$

for $j = 1, 2, \ldots, \bar{K}$. Therefore, for the second layer, we have

$$\lim_{k\to\infty} \|p_{z_j^{(2)}}(kT) - h_{2,\bar{K}-j+1}(kT)\| = 0.$$

Similarly, $\bar{K}$ of the $n - 2\bar{K}$ excess agents will form the third layer of agent array below the second layer. Again, the distance between this third layer and the second layer is s_2. By following the above argument, it is then straightforward to show that there exists a set

$$Z^{(3)} := \{z_1^{(3)}, z_2^{(3)}, \ldots, z_{n_3}^{(3)}\} \subset \{1, 2, \ldots, n\} \setminus (Z^{(1)} \cup Z^{(2)})$$

such that $\lim_{k\to\infty} \|p_{z_j^{(3)}}(kT) - h_{3,j}(kT)\| = 0$, for $j = 1, 2, \ldots, \bar{K}$. Here, agent $z_1^{(3)}$ connects with agent $z_{\bar{K}}^{(2)}$ that is the leftmost agent in the second row of agent array.

Therefore, by repeating the above arguments, there always exists a set $Z^{(i)}$ where

$$Z^{(1)} := \{z_1^{(1)}, z_2^{(1)}, \ldots, z_{\bar{K}}^{(1)}\} \subset \{1, 2, \ldots, n\}, \quad \text{for } i = 1;$$
$$Z^{(i)} := \{z_1^{(i)}, z_2^{(i)}, \ldots, z_{\bar{K}}^{(i)}\} \subset \{1, 2, \ldots, n\} \setminus (Z^{(1)} \cup Z^{(2)} \cup \cdots \cup Z^{(i-1)}) \quad \text{for } i = 2, 3, \ldots, \lfloor n/\bar{K} \rfloor,$$

such that if i is odd, then

$$\lim_{k\to\infty} \|p_{z_j^{(i)}}(kT) - h_{i,j}(kT)\| = 0, \quad j = 1, 2, \ldots, \bar{K};$$

or

$$\lim_{k\to\infty} \|p_{z_j^{(i)}}(kT) - h_{i,n_i-j+1}(kT)\| = 0, \quad j = 1, 2, \ldots, \bar{K}$$

if i is even. Hence, condition (3) is satisfied and this completes the proof of Theorem 3.1. □

References

[1] A. Yamashita, T. Arai, J. Ota, H. Asama, Motion planning of multiple mobile robots for cooperative manipulation and transportation, IEEE Transactions on Robotics and Automation 19 (2) (2003) 223–237.
[2] H. Choset, K. Nagatani, Topological simultaneous localization and mapping (SLAM): toward exact localization without explicit localization, IEEE Transactions on Robotics and Automation 17 (2) (2001) 125–137.
[3] D.W. Gage, Command control for many-robot systems, in: Proceedings of the 19th Annual AUVS Technical Symposium, Hunstville, Alabama, USA, vol. 4, 1992, pp. 22–24.
[4] H. Choset, Coverage for robotics—a survey of recent results, Annals of Mathematics and Artificial Intelligence 31 (1–4) (2001) 113–126.
[5] J. Cortes, S. Martinez, T. Karatas, F. Bullo, Coverage control for mobile sensing networks, IEEE Transactions on Robotics and Automation 20 (2) (2004) 243–255.
[6] T.M. Cheng, A.V. Savkin, A distributed self-deployment algorithm for the coverage of mobile wireless sensor networks, IEEE Communications Letters 13 (11) (2009) 877–879.
[7] T.M. Cheng, A.V. Savkin, Decentralized control for mobile robotic sensor network self-deployment: barrier and sweep coverage problems, Robotica (2010) (in press) doi:10.1017/S0263574710000147.
[8] A. Jadbabaie, J. Lin, A.S. Morse, Coordination of groups of mobile autonomous agents using nearest neighbor rules, IEEE Transactions on Automatic Control 48 (6) (2003) 988–1001.
[9] W. Ren, R.W. Beard, Distributed Consensus in Multi-Vehicle Cooperative Control, Springer, London, 2008.
[10] M.A. Hsieh, V. Kumar, L. Chaimowicz, Decentralized controllers for shape generation with robotic swarms, Robotica 26 (5) (2008) 691–701.
[11] R. Olfati-Saber, J. Fax, R. Murray, Consensus and cooperation in networked multi-agent systems, Proceedings of the IEEE 95 (1) (2007) 215–233.

[12] Y. Hong, G. Chen, L. Bushnell, Distributed observers design for leader-following control of multi-agent networks, Automatica 44 (3) (2008) 846–850.
[13] F. Bullo, J. Cortés, S. Martínez, Distributed Control of Robotic Networks, in: Applied Mathematics Series, Princeton University Press, 2009.
[14] A. Savkin, H. Teimoori, Decentralized formation flocking and stabilization for networks of unicycles, in: Proceedings of the IEEE Conference on Decision and Control, Shanghai, China, 2009, pp. 984–989.
[15] G. Shi, Y. Hong, Global target aggregation and state agreement of nonlinear multi-agent systems with switching topologies, Automatica 45 (5) (2009) 1165–1175.
[16] C.M. Breder, Equations descriptive of fish schools and other animal aggregations, Ecology 35 (3) (1954) 361–370.
[17] E. Shaw, The schooling of fishes, Scientific American 206 (1962) 128–138.
[18] A. Okubo, Dynamical aspects of animal grouping: swarms, schools, flocks, and herds, Advances in Biophysics 22 (1986) 1–94.
[19] K. Warburton, J. Lazarus, Tendency-distance models of social cohesion in animal groups, Journal of Theoretical Biology 150 (4) (1991) 473–488.
[20] G. Flierl, D. Grunbaum, S. Levin, D. Olson, From individuals to aggregations: the interplay between behavior and physics, Journal of Theoretical Biology 196 (1999) 397–454.
[21] T. Vicsek, A. Czirok, E.B. Jacob, I. Cohen, O. Schochet, Novel type of phase transitions in a system of self-driven particles, Physical Review Letters 75 (1995) 1226–1229.
[22] A.V. Savkin, Coordinated collective motion of groups of autonomous mobile robots: analysis of Vicsek's model, IEEE Transactions on Automatic Control 49 (6) (2004) 981–983.
[23] H. Yu, Y. Wang, Coordinated collective motion of groups of autonomous mobile robots with directed interconnected topology, Journal of Intelligent and Robotic Systems 53 (1) (2008) 87–98.
[24] F. Jiang, L. Wang, Finite-time information consensus for multi-agent systems with fixed and switching topologies, Physica D: Nonlinear Phenomena 238 (16) (2009) 1550–1560.
[25] J. Zhang, Y. Zhao, B. Tian, L. Peng, H.-T. Zhang, B.-H. Wang, T. Zhou, Accelerating consensus of self-driven swarm via adaptive speed, Physica A: Statistical Mechanics and its Applications 388 (7) (2009) 1237–1242.
[26] W. Li, X. Wang, Adaptive velocity strategy for swarm aggregation, Physical Review E—Statistical, Nonlinear and Soft Matter Physics 75 (2) (2007).
[27] W. Li, H.-T. Zhang, M. Chen, T. Zhou, Singularities and symmetry breaking in swarms, Physical Review E—Statistical, Nonlinear and Soft Matter Physics 77 (2) (2008).
[28] W. Yang, L. Cao, X. Wang, X. Li, Consensus in a heterogeneous influence network, Physical Review E—Statistical, Nonlinear and Soft Matter Physics 74 (3) (2006).
[29] P. Wang, Navigation strategies for multiple autonomous mobile robots moving in formation, Journal of Robotic Systems 8 (2) (1991) 177–195.
[30] M. Egerstedt, X. Hu, Formation constrained multi-agent control, IEEE Transactions on Robotics and Automation 17 (6) (2001) 947–951.
[31] N. Leonard, E. Fiorelli, Virtual leaders, artificial potentials and coordinated control of groups, in: Proceedings of the IEEE Conference on Decision and Control, vol. 3, 2001, pp. 2968–2973.
[32] V. Gazi, K.M. Passino, A class of attractions/repulsion functions for stable swarm aggregations, International Journal of Control 77 (18) (2004) 1567–1579.
[33] R. Cassinis, G. Bianco, A. Cavagnini, P. Ransenigo, Strategies for navigation of robot swarms to be used in landmines detection, in: Third European Workshop on Advanced Mobile Robots, Eurobot'99, 1999, pp. 211–218.
[34] S. Kumar, T.H. Lai, A. Arora, Barrier coverage with wireless sensors, Wireless Networks 13 (6) (2007) 817–834.
[35] A. Jeremić, A. Nehorai, Design of chemical sensor arrays for monitoring disposal sites on the ocean floor, IEEE Journal of Oceanic Engineering 23 (4) (1998) 334–343.
[36] E. Børhaug, A. Pavlov, K.Y. Pettersen, Straight line path following for formations of underactuated underwater vehicles, in: Proceedings of the 46th IEEE Conference on Decision and Control, New Orleans, USA, 2007, pp. 1905–1912.
[37] P.N. Pathirana, A.V. Savkin, S. Jha, Location estimation and trajectory prediction for cellular networks with mobile base stations, IEEE Transactions on Vehicular Technology 53 (6) (2004) 1903–1913.
[38] P.N. Pathirana, N. Bulusu, A.V. Savkin, S. Jha, Node localization using mobile robots in delay-tolerant sensor networks, IEEE Transactions on Mobile Computing 4 (3) (2005) 285–296.
[39] C.D. Meyer, Matrix Analysis and Applied Linear Algebra, SIAM, Philadelphia, 2000.